Fermi National Accelerator Laboratory

FERMILAB-Pub-93/182-A
astro-ph/9307035
submitted to *Physical Review D*

RECOVERING THE INFLATIONARY POTENTIAL

Michael S. Turner

Departments of Physics and of Astronomy & Astrophysics
Enrico Fermi Institute
The University of Chicago, Chicago, IL 60637-1433

NASA/Fermilab Astrophysics Center
Fermi National Accelerator Laboratory, Batavia, IL 60510-0500

ABSTRACT

A procedure is developed for the recovery of the inflationary potential over the interval that affects astrophysical scales (≈ 1 Mpc-10^4 Mpc). The amplitudes of the scalar and tensor metric perturbations and their power-spectrum indices, which can in principle be inferred from large-angle CBR anisotropy experiments and other cosmological data, determine the value of the inflationary potential and its first two derivatives. From these, the inflationary potential can be reconstructed in a Taylor series and the consistency of the inflationary hypothesis tested. A number of examples are presented, and the effect of observational uncertainties is discussed.

Operated by Universities Research Association Inc. under contract with the United States Department of Energy

1 Introduction

The detection of anisotropy in the cosmic background radiation (CBR) by the Differential Microwave Radiometer on the Cosmic Background Explorer (COBE) satellite [1] has provided the first evidence for the existence of the primeval density perturbations that seeded all the structure seen in the Universe today. Two other experiments have now confirmed the COBE detections [2], and numerous experiments are underway to probe anisotropy on angular scales from arcminutes to tens of degrees. [CBR anisotropy on angular-scale θ arises primarily due to metric perturbations on length-scale $100\,\mathrm{Mpc}\,(\theta/\mathrm{deg})$, so that CBR anisotropy can probe metric fluctuations on scales from about $10\,\mathrm{Mpc}$ to $10^4\,\mathrm{Mpc}$.]

The COBE DMR detection has opened the door for the study of the primeval density perturbations, and thereby the microphysics that produced them. At the moment there are three viable models of structure formation: the cold dark matter models, wherein the perturbations arise from quantum fluctuations excited during inflation and expanded to astrophysical length scales ($t \sim 10^{-34}\,\mathrm{sec}$); the models wherein the seed perturbations are topological defects [3], such as textures, cosmic strings, and global monopoles, produced in a very-early phase transition ($t \sim 10^{-36}\,\mathrm{sec}$); and the PIB model [4], wherein the perturbations are local fluctuations in the baryon number of unknown origin. The PIB model distinguishes itself from the others in requiring no nonbaryonic dark matter ($\Omega_0 = \Omega_B \sim 0.2$).

The cold dark matter models motivated by inflation have been relatively successful, though not without shortcomings [5]. In these models there are, in addition to density (scalar metric) perturbations, gravity-wave (tensor metric) perturbations that also give rise to CBR temperature anisotropy. This is a curse and a blessing: CBR anisotropy cannot be assumed to reflect the underlying density perturbations alone; on the other hand, if the tensor and scalar contributions can be separated, much can be learned about the underlying inflationary potential [6, 7].

The separation of the contribution of scalar and tensor perturbations to CBR anisotropy involves exploiting their different dependencies upon angu-

lar scale and possibly their contributions to the polarization of the CBR anisotropy [8, 9]. In addition, since the scalar perturbations alone seed the formation of structure, measurements of the distribution of matter in the Universe derived from red-shift surveys, peculiar-velocity measurements, and so on can be used to determine their spectrum independently.

The concern of this paper is what can be learned about the inflationary potential from the spectral indices and amplitudes of the scalar and tensor metric perturbations. This question has also been addressed elsewhere [6]; our approach follows the formalism set up in Ref. [7] which is applicable to inflationary potentials that are relatively smooth over the interval that determines metric perturbations on astrophysical scales. It is not applicable to potentials with "specially engineered features" [10].

2 The Method

We use four observables to characterize the scalar and tensor metric perturbations: their contributions to the variance of the CBR quadrupole anisotropy, S for scalar and T for tensor, and the power-law indices of their fluctuation spectra, n for scalar and n_T for tensor. (For scale-invariant perturbations $n = 1$ and $n_T = 0$. The horizon-crossing amplitudes of density perturbations vary with scale as $\lambda^{(1-n)/2}$ and of the gravity-wave perturbations as $\lambda^{-n_T/2}$.)

In Ref. [7] it was shown that these quantities can be related to the value of the inflationary potential, its steepness, and the change in its steepness, evaluated around the epoch that the scales of current astrophysical interest crossed outside the horizon during inflation (about 50 e-folds before the end of inflation):

$$\begin{aligned} V_{50} &\equiv V(\phi_{50}); \\ x_{50} &\equiv \frac{m_{\rm Pl} V'(\phi_{50})}{V_{50}}; \\ x'_{50} &\equiv x'(\phi_{50}) = \frac{m_{\rm Pl} V''(\phi_{50})}{V_{50}} - \frac{x_{50}^2}{m_{\rm Pl}}; \end{aligned} \tag{1}$$

ϕ_{50} is the value of the scalar field that drives inflation 50 e-folds before the

end of inflation (or however many e-folds before the end of inflation the astrophysically relevant scales crossed outside the horizon), $m_{\rm Pl} = 1.22 \times 10^{19}\,{\rm GeV}$ is the Planck mass, and prime indicates derivative with respect to ϕ.

The formulae relating the observables S, T, n, and n_T and the properties of the inflationary potential are

$$\begin{aligned} S \equiv \frac{5\langle|a_{2m}^S|^2\rangle}{4\pi} &= 2.22\frac{V_{50}}{{m_{\rm Pl}}^4 x_{50}^2}\left(1 + 1.1(n-1) + \frac{7}{6}[n_T - (n-1)]\right); \\ T \equiv \frac{5\langle|a_{2m}^T|^2\rangle}{4\pi} &= 0.606\frac{V_{50}}{{m_{\rm Pl}}^4}(1 + 1.2 n_T); \\ n &= 1 - \frac{x_{50}^2}{8\pi} + \frac{m_{\rm Pl} x'_{50}}{4\pi}; \\ n_T &= -\frac{x_{50}^2}{8\pi}; \\ \frac{T}{S} &= 0.28 x_{50}^2 = -7\, n_T; \end{aligned} \tag{2}$$

where S (T) is the contribution of scalar (tensor) perturbations to the variance of the CBR quadrupole temperature anisotropy and brackets indicate the ensemble average [13]. Since the four observables can be expressed in terms of three properties of the potential a consistency check exists [7].

These formulae have been computed to lowest order in the deviation from scale invariance, i.e., $\mathcal{O}(n_T, n-1)$, and only apply to smooth potentials. Note too that n_T must be less than zero (more power on large scales), though the scalar power-law index n can be greater than 1. From Eqs. (2) one can solve for the potential and its first two derivatives:

$$\begin{aligned} V_{50} &= 1.65\, T\,(1 - 1.2 n_T); \\ V'_{50} &= 5.01\sqrt{-n_T}\,(V_{50}/m_{\rm Pl}); \\ V''_{50} &= 4\pi\left[(n-1) - 3n_T\right]\,(V_{50}/{m_{\rm Pl}}^2). \end{aligned} \tag{3}$$

At present, the COBE DMR detection serves mainly to determine the

sum of the scalar and tensor contributions to the quadrupole anisotropy:[1]

$$T + S = \left(\frac{16 \pm 4\,\mu\mathrm{K}}{2.726\,\mathrm{K}}\right)^2 \simeq 3.4 \times 10^{-11}. \tag{4}$$

In Ref. [7] detailed formulae for the tensor and scalar contributions to the higher multipoles are given; very roughly, for $l \ll 200$ and standard recombination,

$$\begin{aligned} \frac{l(l+1)\langle|a_{lm}^S|^2\rangle}{4\pi} &\sim S\,(l/2)^{n-1}; \\ \frac{l(l+1)\langle|a_{lm}^T|^2\rangle}{4\pi} &\sim T\,(l/2)^{n_T}. \end{aligned} \tag{5}$$

Thus, in principle, a separation of the tensor and scalar contributions to the individual multipole amplitudes determines n_T and $n-1$. Since n_T is directly related to the ratio of the tensor to scalar contributions of the quadrupole anisotropy, measurements of S and T also determines n_T.

The recovery of the inflationary potential proceeds by constructing its Taylor series:

$$V(\phi) = V_{50} + (\phi - \phi_{50})\,V'_{50} + (\phi - \phi_{50})^2\,V''_{50}/2! + \cdots; \tag{6}$$

as before, ϕ_{50} is the value of the scalar field 50 e-folds before the end of inflation. Measurements of T, S, n, and n_T only determine the square of V'_{50}, so the sign of V'_{50} cannot be determined; as a matter of convention we always take it to be negative. The sign of V' is not physical since it can be changed by the field redefinition: $\phi \to -\phi$.

Scalar and tensor metric perturbations on the astrophysically relevant scales—say from the scale of galaxies, about 1 Mpc, to the present horizon scale, $H_0^{-1} \sim 10^4\,\mathrm{Mpc}$—were created during a small portion of the inflationary epoch, corresponding to an interval of roughly 8 e-folds around 50 e-folds before the end of inflation (a precise formula relating the epoch when

[1]The value for the variance of the CBR quadrupole anisotropy derived from the COBE DMR data depends slightly upon the spectral index of the metric perturbations; see Refs. [1].

a scale went outside the horizon during inflation and the parameters of inflation is given in Ref. [7]). This means that astrophysical and cosmological data can only reveal information about the inflationary potential over this narrow interval, a fact which motivated the formalism developed in [7]. As a matter of principle, we will only reconstruct the potential over the interval that corresponds to these 8 e-foldings of the scale factor.

The equation of motion for ϕ in the slow-rollover approximation [11], $\dot{\phi} = -V'/3H$, can be recast as

$$\frac{d\phi}{dN} = \frac{m_{\rm Pl} x}{8\pi}; \tag{7}$$

where N is the number of e-folds before the end of inflation. By expanding the steepness x around ϕ_{50}, $x(\phi) = x_{50} + (\phi - \phi_{50})x'_{50}$, one obtains ϕ as a function of N:

$$\begin{aligned} \phi - \phi_{50} &= \frac{x_{50}}{x'_{50}} \left(\exp[(N-50) m_{\rm Pl} x'_{50}/8\pi] - 1\right); \\ &= \frac{m_{\rm Pl}\sqrt{-n_T/2\pi}}{n-1-n_T} \left(\exp[(N-50)(n-1-n_T)/2] - 1\right). \end{aligned} \tag{8}$$

The change in the value of the scalar field over the 8 important e-folds of inflation ($= \Delta\phi$) depends upon n and n_T: If the difference between $n-1$ and n_T is very small, then $\Delta\phi \sim \sqrt{-n_T} m_{\rm Pl}$; on the other hand, if $\sqrt{-n_T}$ is very small or the difference between $n-1$ and n_T is large, then $\Delta\phi$ is much less than $m_{\rm Pl}$.

This equation, together with the Taylor expansion for the potential, cf. Eq. (6), and the equations relating V_{50}, V'_{50}, and V''_{50} to the observables S, T, n, and n_T, cf. Eqs. (3), are all we need to recover the inflationary potential. To begin, we will recover some familiar inflationary potentials which have been analyzed elsewhere in the formalism discussed above [7]. For these potentials we do not worry about the scale of inflation, V_{50}, which is set measurements of S and T (see below); we will only be interested in the shape of the potential. Specifying n_T and n is sufficient to recover the shape, though we also give T/S as it may be easier to measure than n_T (and of course is equivalent to n_T).

3 Some Examples

3.1 Familiar potentials

First, consider potentials of the form $V(\phi) = a\phi^b$, often used in models of chaotic inflation [12]. For these models [7]

$$T/S = 0.07b; \qquad n_T = -0.01b; \qquad n = 0.98 - 0.01b.$$

Note, the deviations from scale invariance increase with b; since our recovery process involves an expansion in the deviation from scale invariance one expects the recovery of the potential to be less accurate for larger values of b. In Figs. 1 we show the original potential and the recovered potential for $b = 2, 4, 16$; even for $b = 16$ the recovery is quite accurate.

Next, consider exponential potentials, $V(\phi) = V_0 \exp(-\beta\phi/m_{\rm Pl})$, which arise in models of extended inflation [14]. For these models [7]

$$T/S = 0.28\beta^2; \qquad n_T = -\frac{\beta^2}{8\pi}; \qquad n - 1 = n_T.$$

In Figs. 2 we show the reconstruction for $\beta = 1.23, 1.94, 6.03$, corresponding to $n_T = -0.06, -0.15, -0.24$. Only for $n_T = -0.24$ is the recovery of the potential less excellent: however, this much deviation from scale invariance is probably inconsistent with models of structure formation [15].

Now, consider a cosine potential, $V(\phi) = \Lambda^4[1 + \cos(\phi/f)]$, the type of potential employed in the "natural-inflation" models [16]. It is not possible to provide a general formula for n_T, n, and T/S; however, there are two limiting regimes: $f \gtrsim m_{\rm Pl}$ and $f \lesssim m_{\rm Pl}$. In the first regime, the cosine potential reduces to the case of chaotic inflation with $b = 2$. In the second regime [7],

$$\frac{T}{S} = 0.07 \left(\frac{m_{\rm Pl}}{f}\right)^2 \left(\frac{\phi_{50}}{f}\right)^2 \ll 1; \qquad n = 1 - \frac{1}{8\pi}\left(\frac{m_{\rm Pl}}{f}\right)^2;$$

where $\phi_{50}/f \simeq \pi \exp(-50 m_{\rm Pl}{}^2/16\pi f^2)$. In Fig. 3 we show the recovered potential for $f = m_{\rm Pl}/2$, where $n = 0.84$. Again, the recovery process works very well.

Finally, consider the Coleman-Weinberg potentials, $V(\phi) = B\sigma^4/2 + B\phi^4[\ln(\phi^2/\sigma^2) - 0.5]$, often used in models of new inflation; for these models

$$\frac{T}{S} \simeq 3 \times 10^{-5} \left(\frac{\sigma}{m_{\rm Pl}}\right)^4; \qquad n = 0.94.$$

These potentials are extremely flat and easily recovered as shown in Fig. 4.

3.2 Unknown potentials

Now we turn to the recovery of an unknown potential from cosmological data. The recovery process requires knowledge of three of the quantities T, S, n, and n_T; we will use $T + S$, T/S, and n, which are probably the easiest to measure. The quadrupole temperature anisotropy measures $S+T$; supposing that its value is $16\,\mu$K, the COBE DMR determination, we can immediately infer V_{50}:

$$V_{50} = (3.3 \times 10^{16}\,{\rm GeV})^4 \left(\frac{1 - 1.1(n-1) + \frac{7}{6}(n - 1 - n_T)}{1 + S/T}\right). \qquad (9)$$

(We remind the reader that $n_T = -0.14T/S$.) From this equation we see that the value of V_{50} is most sensitive to T/S, varying inversely with it. That is, the scale of inflation rises with the amplitude of tensor perturbations, asymptotically approaching an energy scale of about 3×10^{16} GeV.

Once V_{50} is fixed, n and T/S determine the shape of the potential. Generically, there are four qualitatively different outcomes for the measured quantities which lead to four generic inflationary potentials:

1. $n \approx 1$ and T/S very small, corresponding to scale-invariant scalar and tensor perturbations

2. n significantly less than 1 and T/S very small, corresponding to tilted scalar fluctuations and scale-invariant, small-amplitude gravity waves

3. $n \approx 1$ and T/S of order unity, corresponding to scale-invariant scalar perturbations and tilted, large-amplitude gravity waves

4. n significantly less than 1 and T/S of order unity, corresponding to tilted scalar and tensor perturbations and large-amplitude gravity waves

The four generic potentials are illustrated in Figs. 5. For large T/S, cases (3) and (4), the potential is steep, the scale of inflation is relatively large, and the variation of ϕ over the relevant 8-folds is of the order of the Planck mass. For small T/S, cases (1) and (2), the potential is very flat, the scale of inflation is relatively low, and the variation of ϕ over the relevant 8-folds is much less than the Planck mass. Coleman-Weinberg potentials provide an example of case (1); cosine potentials and the potential $V(\phi) = -m^2\phi^2 + \lambda\phi^4$ [11] provide examples of case (2); recently, an example of a potential corresponding to case (3) has been presented [17]; and exponential potentials provide an example of case (4). Finally, n can be larger than unity; however, the two new cases, n significantly greater than one and T/S small or of order unity, are qualitatively similar to cases (2) and (4).

4 Discussion

The scalar and tensor contributions to the CBR quadrupole anisotropy, S and T, and the power-law indices of the spectra of scalar and tensor perturbations, n and n_T, serve to determine—indeed overdetermine—the value of the inflationary potential and its first two derivatives. In principle, measurements of these four quantities can be used both to test the consistency of the inflationary hypothesis and to recover the inflationary potential through the first three terms in its Taylor expansion. We have shown the recovery of several familiar potentials, cf. Figs. 1-4, and the four generic types of inflationary potentials that arise, cf. Figs. 5.

In order to recover the inflationary potential measurements of at least three of the quantities n, T, S, and n_T are required. In all likelihood the first three will be the easiest to determine; CBR anisotropy as well as determinations of the distribution of matter and large-scale structure should serve to measure n, and large-angle CBR anisotropy should determine S and T (in the case of T, at least an upper limit). An independent measurement of n_T

seems much more difficult, but provides an important consistency check.

In any case, determinations of n, S, and T are likely to have significant uncertainties, so that the recovery of the underlying inflationary potential will not be as easy or precise as our examples would indicate. In Fig. 6, we show the effect of these uncertainties on the recovery of the shape of the inflationary potential for the following data: $n = 0.9 \pm 0.2$ and $T/S = 0.3 \pm 0.25$. Even worse is the effect of uncertainties on determining the scale of the potential: Recall, when $S+T$ is normalized to the COBE result, V_{50} varies as the inverse of T/S, which for the above "data" leads to an order of magnitude range in the value of V_{50}.

An accurate recovery of the inflationary potential is still a long way from reality—and, of course, it may be that inflation never even occurred. However, with the COBE DMR anisotropy measurements the first step has been taken. Moreover, the potential payoff—probing physics at unification energy scales—is worth the effort, if not the wait.

This work was supported in part by the DOE (at Chicago and Fermilab) and by the NASA through NAGW-2381 (at Fermilab). This work was completed at the Aspen Center for Physics.

References

[1] G. Smoot et al., *Astrophys. J.* **396**, L1 (1992); E.L. Wright et al., *ibid*, L13 (1992).

[2] K. Ganga, E.S. Cheng, S.S. Meyer, and L.A. Page, *Astrophys. J.*, in press (1993); R.A. Watson et al., *Nature* **357**, 660 (1992); R.D. Davies et al., Univ. of Manchester preprint (1993).

[3] N. Turok, *Phys. Rev. Lett.* **63**, 2652 (1989); N. Turok and D. Spergel, *ibid* **64**, 2736 (1990); A. Albrecht and A. Stebbins, *ibid* **69**, 2615 (1992); D. Bennett, A. Stebbins, and F. Bouchet, *Astrophys. J.* **399**, L5 (1992); U. Pen, D. Spergel, and N. Turok, Princeton Univ. preprint (1993).

[4] P.J.E. Peebles, *Nature* **327**, 210 (1987); *Astrophys. J.* **315**, L73 (1987); R. Cen, J.P. Ostriker, and P.J.E. Peebles, *Astrophys. J.*, in press (1993).

[5] J.P. Ostriker, *Ann. Rev. Astron. Astrophys.* **31**, in press (1993); M.S. Turner, in *Proceedings of TASI-92*, eds. J.A. Harvey and J. Polchinski (WSPC, Singapore, 1993).

[6] H.M. Hodges and G.R. Blumenthal, *Phys. Rev. D* **42**, 3329 (1990); E. Copeland et al., *Phys. Rev. Lett.* **71**, 219 (1993).

[7] M.S. Turner, *Phys. Rev. D*, in press (1993).

[8] R. Davis et al., *Phys. Rev. Lett.* **69**, 1856 (1992).

[9] R. Crittenden et al., *Phys. Rev. Lett.*, in press (1993); R. Crittenden, R. Davis, and P.J. Steinhardt, astro-ph/9306027 (1993).

[10] See e.g., D. Salopek, J.R. Bond, and J.M. Bardeen, *Phys. Rev. D* **40**, 1753 (1989); H.M. Hodges, G.R. Blumenthal, J.R. Primack, and L. Kofman, *Nucl. Phys. B* **335**, 197 (1990).

[11] P.J. Steinhardt, *Phys. Rev. D* **29**, 2162 (1984).

[12] A.D. Linde, *Phys. Lett. B* **129**, 177 (1983); V. Belinsky, L. Grishchuk, I. Khalatanikov, and Ya.B. Zel'dovich, *ibid* **155**, 232 (1985).

[13] M.S. Turner, M. White, and J. Lidsey, astro-ph/9306029.

[14] D. La and P.J. Steinhardt, *Phys. Rev. Lett.* **62**, 376 (1989); E.W. Kolb, D. Salopek, and M.S. Turner, *Phys. Rev. D* **42**, 3925 (1990).

[15] F. Adams et al., *Phys. Rev. D* **47**, 426 (1993); J. Gelb et al., *Astrophys. J.* **403**, L5 (1993); R. Cen et al., *ibid* **399**, L11 (1992).

[16] K. Freese, J. Frieman, and A. Olinto, *Phys. Rev. Lett.* **65**, 3233 (1990).

[17] J.D. Barrow and A.R. Liddle, *Phys. Rev. D* **47**, R5219 (1993).

FIGURE CAPTIONS

Figure 1: Recovery of chaotic potentials, $V(\phi) = a\phi^b$, over the 8 e-folds relevant for astrophysical scales and for comparison the original potential (broken curves): (a) $b = 2$; (b) $b = 4$; and (c) $b = 16$.

Figure 2: Recovery of exponential potentials, $V(\phi) = V_0 \exp(-\beta\phi/m_{\rm Pl})$, and for comparison the original potential (broken curves): (a) $\beta = 1.23$; (b) $\beta = 1.94$; and (c) $\beta = 6.03$.

Figure 3: Recovery of the cosine potential, $V(\phi) = \Lambda^4[1 + \cos(\phi/f)]$ and $f = m_{\rm Pl}/2$, and for comparison the original potential (broken curve).

Figure 4: Recovery of a Coleman-Weinberg potential with $\sigma = 1 \times 10^{16}$ GeV and for comparison the original potential (broken curve).

Figure 5: The four generic inflationary potentials: (a) $n-1 = -2\times10^{-6}$ and $T/S = 1.4\times10^{-5}$, with the COBE DMR normalization $V_{50}^{1/4} = 2.0\times10^{15}$ GeV; (b) $n = 0.85$ and $T/S = 1.4 \times 10^{-4}$, $V_{50}^{1/4} = 3.6 \times 10^{15}$ GeV; (c) $n = 1$ and $T/S = 1$, $V_{50}^{1/4} = 2.9 \times 10^{16}$ GeV; and (d) $n = 0.85$ and $T/S = 1$, $V_{50}^{1/4} = 2.9 \times 10^{16}$ GeV.

Figure 6: An illustration of the effect of observational uncertainties on the shape of the recovered potential; here $n = 0.9 \pm 0.2$ and $T/S = 0.3 \pm 0.25$. The four curves correspond to $n = 0.7$ and $T/S = 0.05$ (solid), $n = 0.7$ and $T/S = 0.55$ (dotted), $n = 1.1$ and $T/S = 0.05$ (dashed), and $n = 1.1$ and $T/S = 0.55$ (long-dashed).

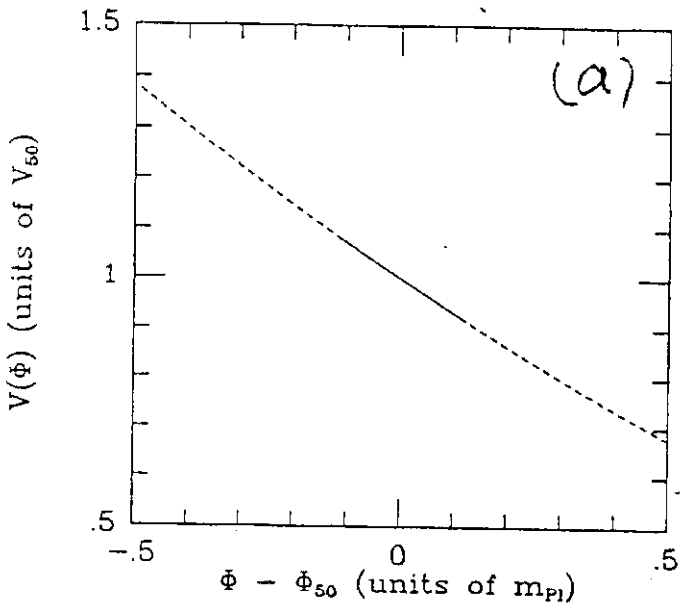
(a)
1.5
1
.5
−.5
0
.5
V(Φ) (units of V50)
Φ − Φ50 (units of mPl)

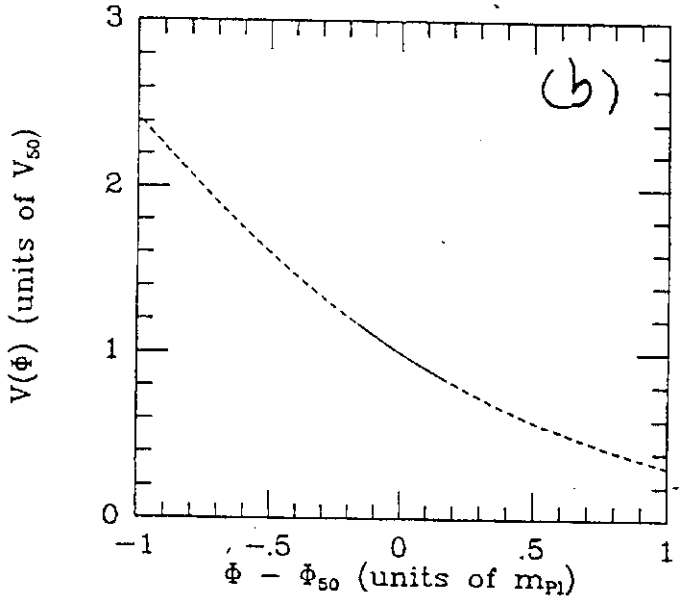
(b)
3
2
1
0
−1
−.5
0
.5
1
V(Φ) (units of V50)
Φ − Φ50 (units of mPl)

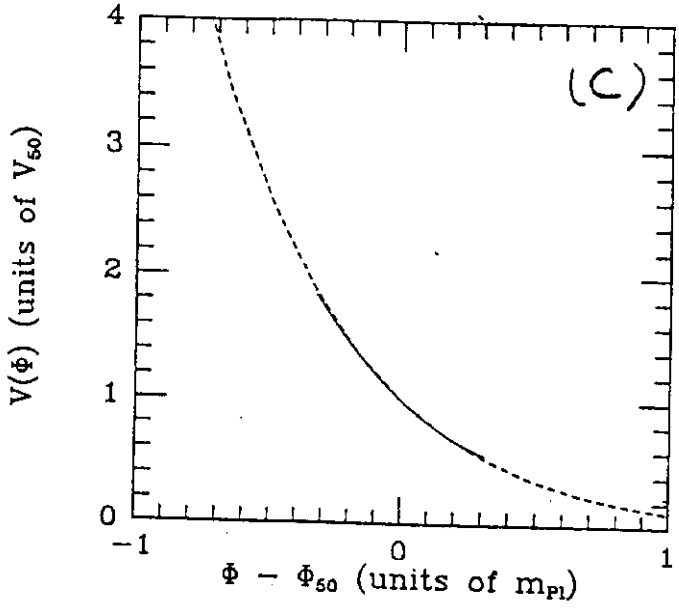
(c)
4
3
2
1
0
−1
0
1
V(Φ) (units of V50)
Φ − Φ50 (units of mPl)

- FIG 1 -

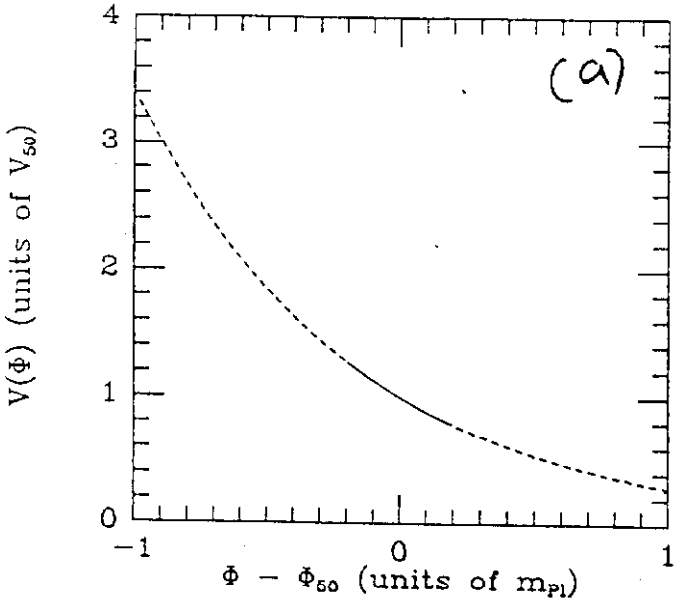
(a)
V(Φ) (units of V50)
Φ − Φ50 (units of mPl)
0
1
2
3
4
−1
0
1

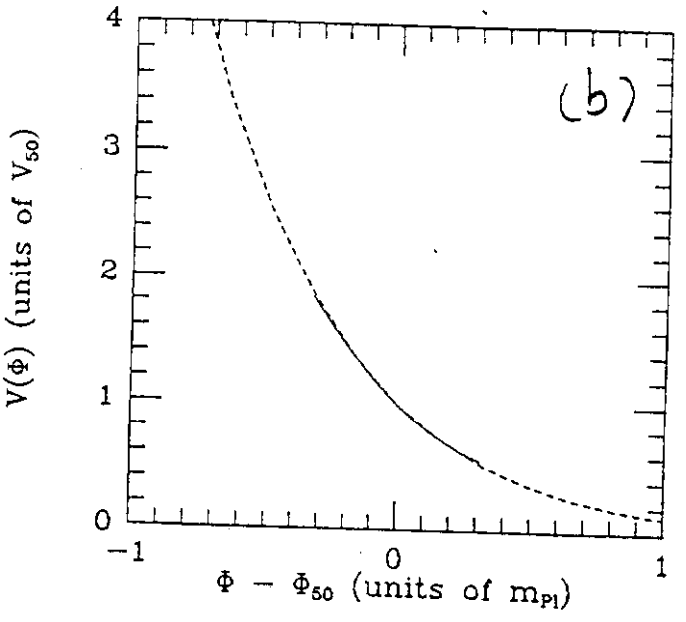
(b)
V(Φ) (units of V50)
Φ − Φ50 (units of mPl)
0
1
2
3
4
−1
0
1

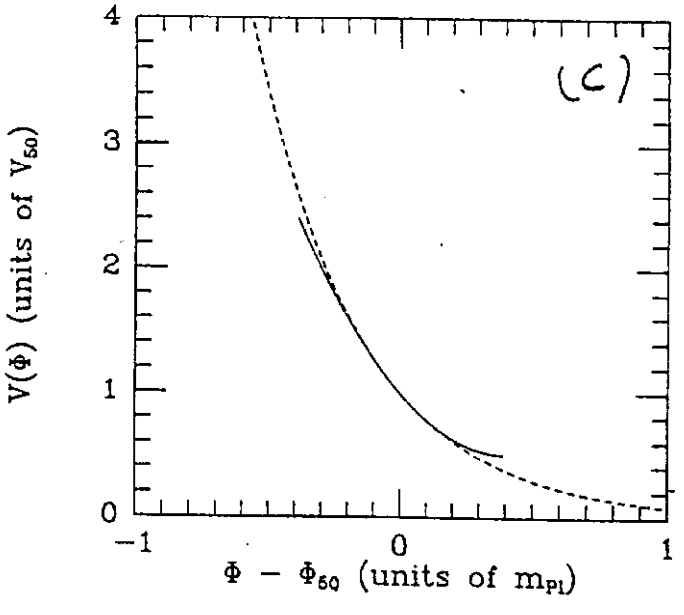
(c)
V(Φ) (units of V50)
Φ − Φ50 (units of mPl)
0
1
2
3
4
−1
0
1

– FIG 2 –

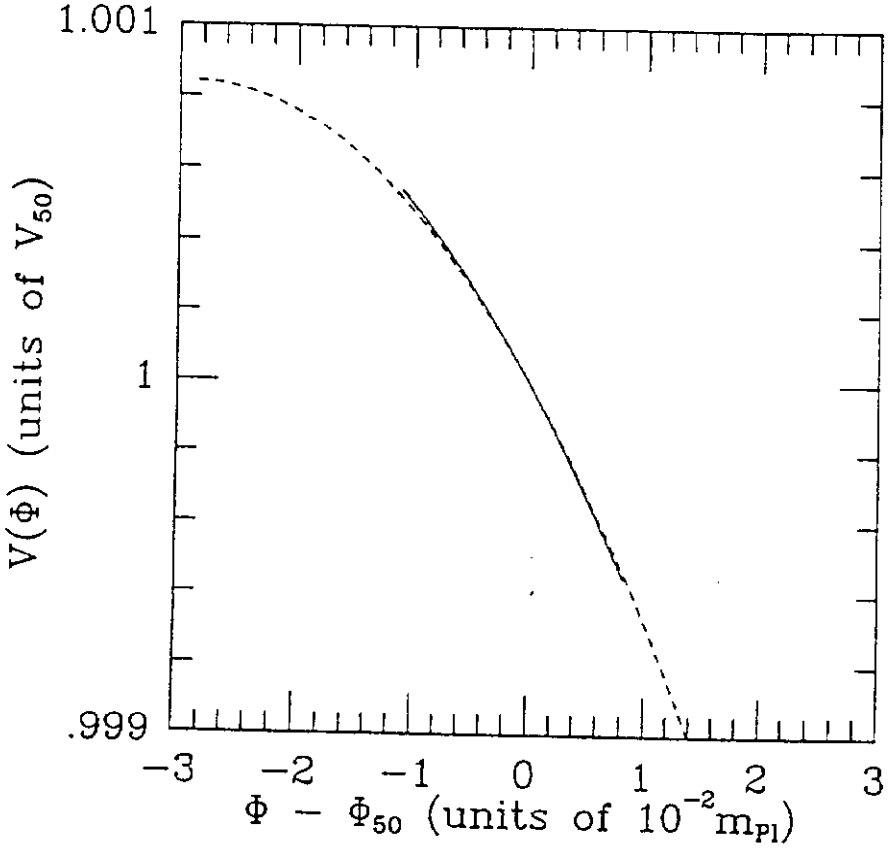
1.001
1
.999
$V(\Phi)$ (units of V_{50})
−3
−2
−1
0
1
2
3
$\Phi - \Phi_{50}$ (units of $10^{-2} m_{Pl}$)

– FIG 3 –

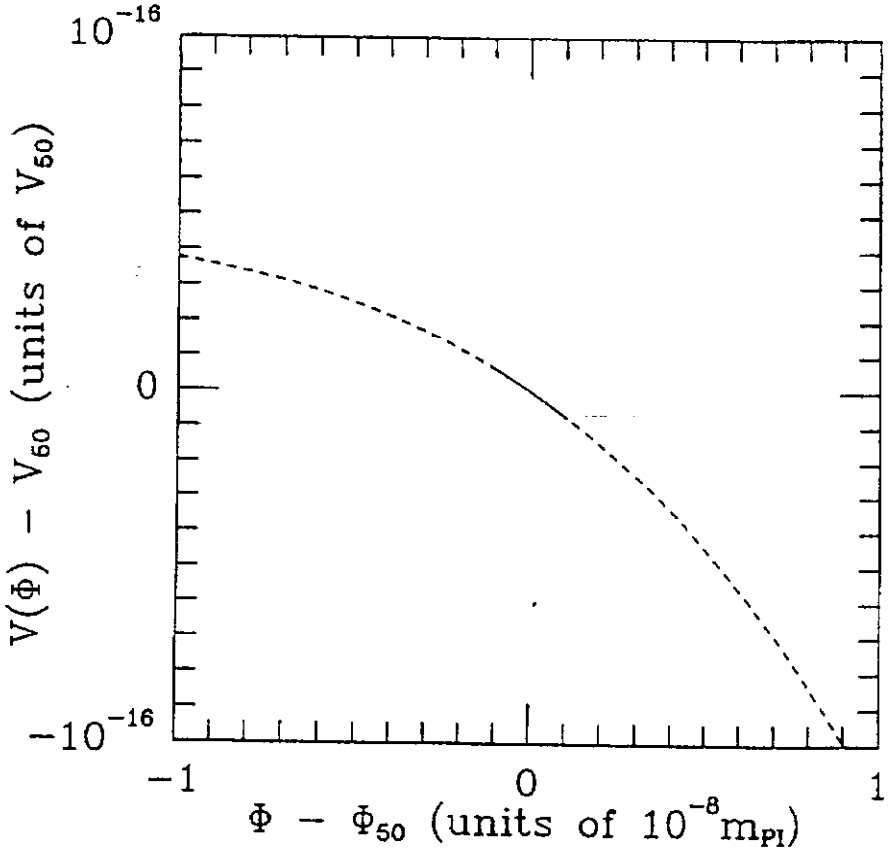
10^{-16}
0
-10^{-16}
$V(\Phi) - V_{60}$ (units of V_{60})
−1
0
1
$\Phi - \Phi_{50}$ (units of $10^{-8} m_{Pl}$)

– FIG 4 –

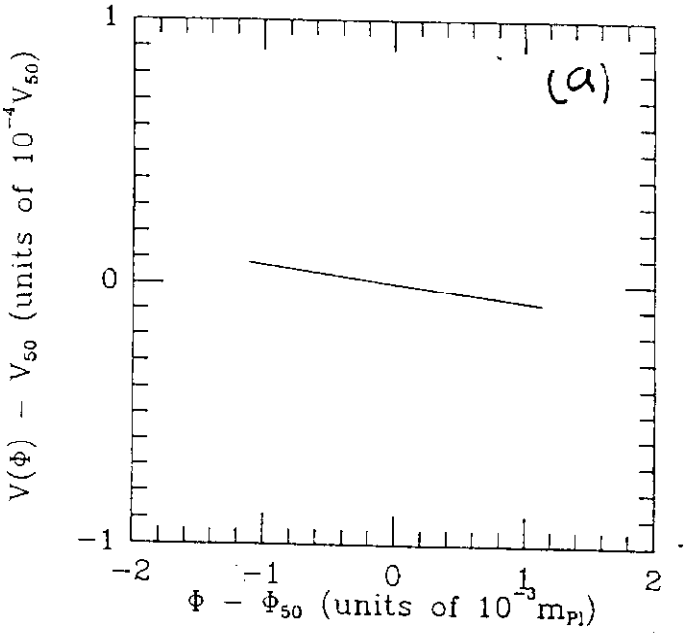
(a)
1
0
−1
−2
−1
0
1
2
V(Φ) − V50 (units of 10⁻⁴V50)
Φ − Φ50 (units of 10⁻³mPl)

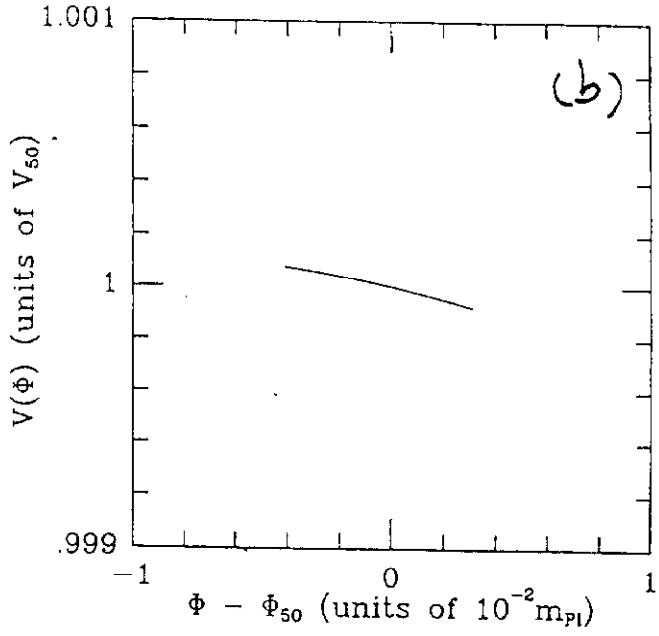
(b)
1.001
1
.999
−1
0
1
V(Φ) (units of V50)
Φ − Φ50 (units of 10⁻²mPl)

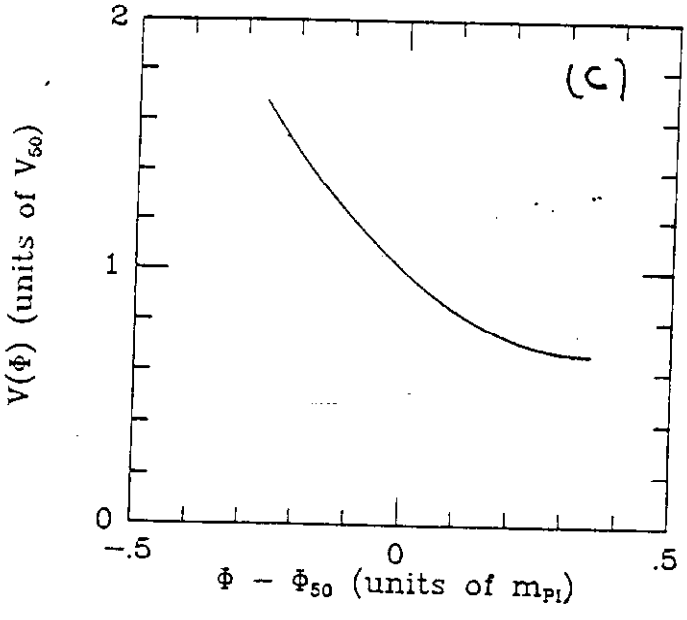
(c)
2
1
0
−.5
0
.5
V(Φ) (units of V60)
Φ − Φ50 (units of mPl)

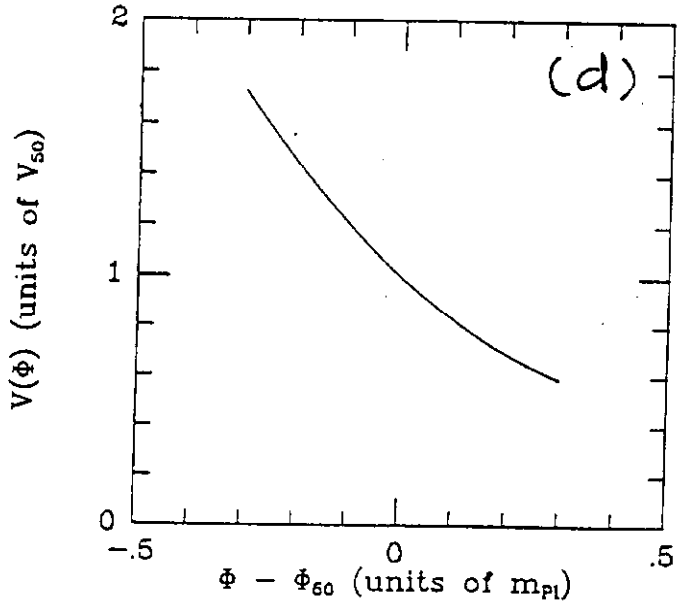
(d)
2
1
0
−.5
0
.5
V(Φ) (units of V50)
Φ − Φ60 (units of mPl)

- FIG 5 -

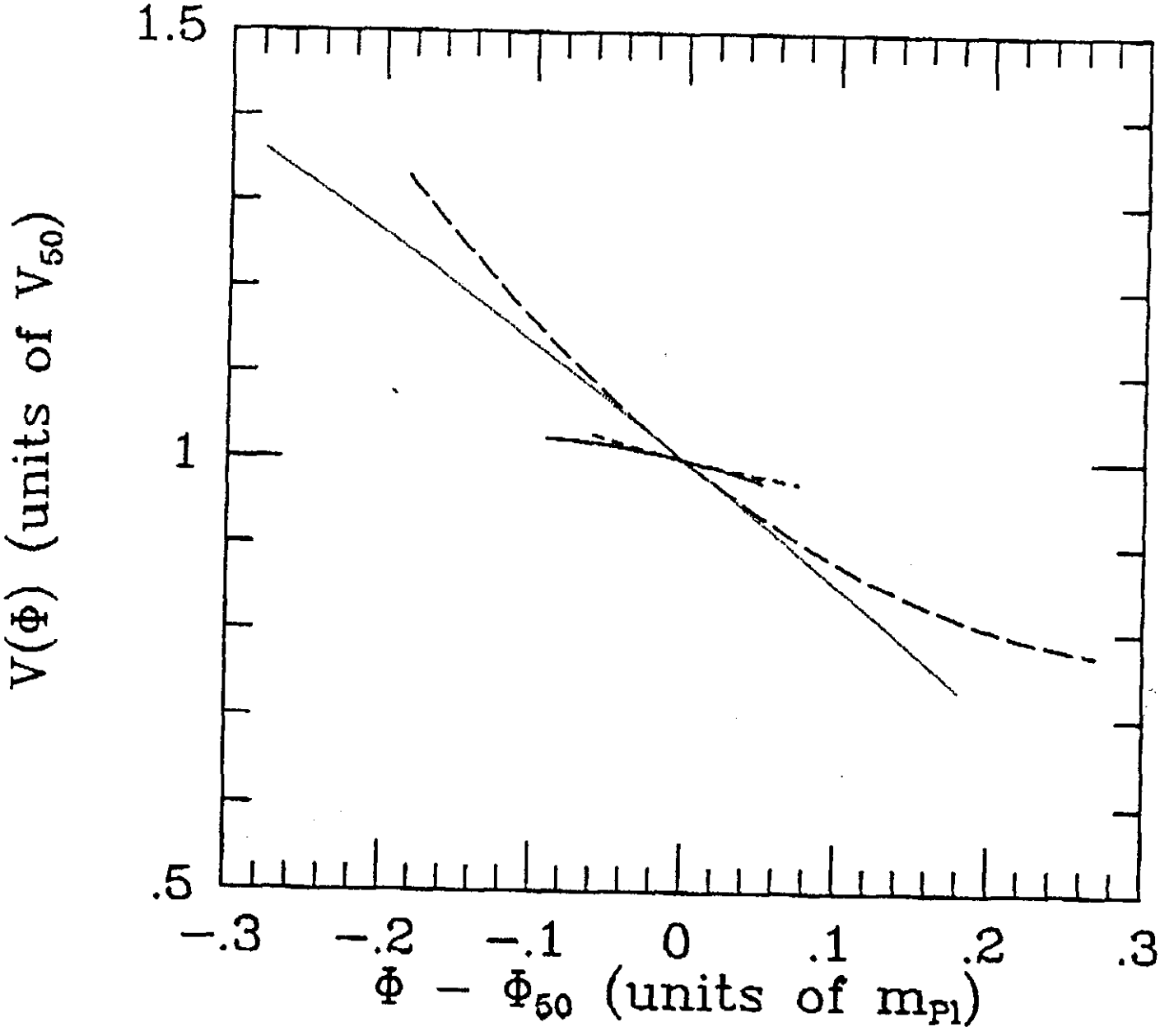

– FIG 6 –